Biogeosciences

Open Access

Effects of low oxygen concentrations on aerobic methane oxidation in seasonally hypoxic coastal waters

Lea Steinle[1,2]**, Johanna Maltby**[2,3]**, Tina Treude**[2,4]**, Annette Kock**[2]**, Hermann W. Bange**[2]**, Nadine Engbersen**[1]**, Jakob Zopfi**[1]**, Moritz F. Lehmann**[1]**, and Helge Niemann**[1,5]

[1]Department of Environmental Sciences, University of Basel, 4056 Basel, Switzerland
[2]GEOMAR Helmholtz Centre for Ocean Research Kiel, Marine Biogeochemistry Research Division, 24148 Kiel, Germany
[3]Department of Natural Sciences, Saint Joseph's College, Standish, Maine, USA
[4]Department of Earth, Planetary & Space Sciences and Atmospheric & Oceanic Sciences, University of Los Angeles, Los Angeles, California, USA
[5]CAGE – Centre for Arctic Gas Hydrate, Environment and Climate, Department of Geology, UiT the Arctic University of Norway, 9037 Tromsø, Norway

Correspondence to: Lea Steinle (lea.steinle@unibas.ch)

Abstract. Coastal seas may account for more than 75 % of global oceanic methane emissions. There, methane is mainly produced microbially in anoxic sediments from which it can escape to the overlying water column. Aerobic methane oxidation (MOx) in the water column acts as a biological filter, reducing the amount of methane that eventually evades to the atmosphere. The efficiency of the MOx filter is potentially controlled by the availability of dissolved methane and oxygen, as well as temperature, salinity, and hydrographic dynamics, and all of these factors undergo strong temporal fluctuations in coastal ecosystems. In order to elucidate the key environmental controls, specifically the effect of oxygen availability, on MOx in a seasonally stratified and hypoxic coastal marine setting, we conducted a 2-year time-series study with measurements of MOx and physicochemical water column parameters in a coastal inlet in the south-western Baltic Sea (Eckernförde Bay). We found that MOx rates generally increased toward the seafloor, but were not directly linked to methane concentrations. MOx exhibited a strong seasonal variability, with maximum rates (up to 11.6 nmol L^{-1} d^{-1}) during summer stratification when oxygen concentrations were lowest and bottom-water temperatures were highest. Under these conditions, 2.4–19.0 times more methane was oxidized than emitted to the atmosphere, whereas about the same amount was consumed and emitted during the mixed and oxygenated periods. Laboratory experiments with manipulated oxygen concentrations in the range of 0.2–220 µmol L^{-1} revealed a submicromolar oxygen optimum for MOx at the study site. In contrast, the fraction of methane–carbon incorporation into the bacterial biomass (compared to the total amount of oxidized methane) was up to 38-fold higher at saturated oxygen concentrations, suggesting a different partitioning of catabolic and anabolic processes under oxygen-replete and oxygen-starved conditions, respectively. Our results underscore the importance of MOx in mitigating methane emission from coastal waters and indicate an organism-level adaptation of the water column methanotrophs to hypoxic conditions.

1 Introduction

Methane is a potent greenhouse gas, but the contributions of individual natural sources to the atmospheric budget are still not well constrained (Kirschke et al., 2013). Coastal (shelf) seas are estimated to account for more than 75 % of the global marine methane emissions, even though they cover only about 15 % of the total ocean surface area (Bange et al., 1994; Bakker et al., 2014). In coastal systems, methane is mainly produced via degradation of organic matter by methanogenic archaea in anoxic sediments (Ferry, 1993; Bakker et al., 2014). Part of the produced methane is con-

sumed via anaerobic or aerobic oxidation of methane within the sediments (Knittel and Boetius, 2009; Boetius and Wenzhöfer, 2013), but a significant fraction often escapes into the overlying water column (Reeburgh, 2007). In the water column, methane can also be oxidized anaerobically in the case of water column anoxia, but most of it is consumed via aerobic oxidation of methane (MOx; R1), mediated by aerobic methane-oxidizing bacteria (MOB; Reeburgh, 2007).

$$CH_4 + 2O_2 \rightarrow CO_2 + 2H_2O \qquad (R1)$$

MOx is hence an important sink for methane before its potential release into the atmosphere, but little is known about the efficiency of MOx in shallow coastal ecosystems, where the distance between the sediment source and the atmosphere is short, leaving little time for exhaustive methane oxidation during vertical advective or turbulent-diffusive transport. Coastal ecosystems undergo large temporal variations, for example, with regard to temperature, oxygen, salinity, or organic matter input (e.g. Lennartz et al., 2014; Gelesh et al., 2016). Additionally, over the past decades, the number of seasonally or permanently hypoxic or even anoxic coastal zones has increased worldwide, most often as a consequence of anthropogenic eutrophication and/or climate change (Diaz and Rosenberg, 2008; HELCOM: 2009; Rhein et al., 2013; Lennartz et al., 2014; Rabalais et al., 2014). Model results also predict that such oxygen-depleted zones will expand in the future since increasing surface water temperatures will lead to enhanced stratification and, thus, to less oxygen supply to bottom waters (Keeling et al., 2010; Friedrich et al., 2014). Several definitions for water column oxygenation levels were suggested in the literature (Diaz and Rosenberg, 2008; Canfield and Thamdrup, 2009; Middelburg and Levin, 2009; Naqvi et al., 2010). Here, we adopt the threshold adapted by Middelburg and Levin (2009) and Naqvi et al. (2010), where hypoxia is defined as $[O_2] < 63 \, \mu mol \, L^{-1}$.

Multiple environmental factors can affect MOx in seasonally stratified coastal marine environments. Oxygen concentrations, for instance, are likely to impact MOx, which is an aerobic or, in some cases, a micro-aerobic process (Carini et al., 2005; Schubert et al., 2006; Blees et al., 2014). Hence, the organic matter flux and, consequently, the rate of oxygen consumption due to organic matter remineralisation may influence how much methane is oxidized via MOx. Enhanced organic matter input can also increase methane production rates (Maltby, 2015), which in turn may stimulate MOx rates. Moreover, increasing ocean water temperatures as a result of climate change may directly impact metabolic rates of microbes, e.g. methanogens or methanotrophs (Madigan et al., 2015). Increasing surface water temperature could also have an indirect effect on MOx, as it will influence water column stratification and thus oxygenation levels during summer time (Diaz and Rosenberg, 2008; Keeling et al., 2010; Friedrich et al., 2014). Finally, water mass circulation, transporting methanotrophs to or away from methane sources can also affect MOx rates (Steinle et al., 2015). In order to predict

the fate of coastal methane, knowledge of the seasonality of water column methane oxidation, and the environmental controls thereupon, are of great importance for predicting future changes in methane emissions (Bakker et al., 2014).

The seasonally hypoxic Boknis Eck time series station located in Eckernförde Bay (SW Baltic Sea) is an excellent site for investigating coastal water column MOx under different oxidation/stratification regimes (see e.g. Bange et al., 2010). Here, we present results from a 2-year study, during which we investigated MOx rates, methane concentrations, and physicochemical parameters in the water column at Boknis Eck on a quarterly basis. The aim was to assess seasonal dynamics of, and the environmental controls on, MOx in this coastal inlet. Combining field observations and laboratory experiments, we specifically addressed the role of oxygen as a modulator of MOx by determining minimum oxygen requirements and potential oxygen concentration optima.

2　Materials and methods

2.1　Site description

The time-series station Boknis Eck (54°31.15 N, 10°02.18 E; www.bokniseck.de; Fig. 1) is situated at the entrance of the coastal inlet Eckernförde Bay in the SW Baltic Sea, with an approximate water depth of 28 m at the sampling site (Bange et al., 2011). Physico-chemical water column parameters have been measured regularly since 1957, making this station one of the longest-operated marine time-series stations worldwide (Lennartz et al., 2014). The hydrography of Eckernförde Bay is characterized by the outflow of low-salinity Baltic Sea water and the inflow of higher-salinity North Sea water through the Kattegat and the Great Belt. From mid-March to mid-September, the water column is stratified with a pycnocline at ∼ 15 m water depth (Lennartz et al., 2014). Large phytoplankton blooms generally occur in early spring (February–March) and in autumn (September–November), and minor blooms occasionally occur during summer (July–August; Smetacek et al., 1984; Smetacek 1985; Bange et al., 2010). The resulting high organic matter fluxes and respiration rates result in a high oxygen demand and, as a consequence, in bottom-water hypoxia (or occasionally even anoxia) during summer (Hansen et al., 1999). The frequency of water column hypoxia in Eckernförde Bay has increased since the 1960s (Lennartz et al., 2014). The high organic matter sinking flux and rapid sedimentation of organic matter also lead to enhanced methanogenesis in the muddy sediment, and to high methane concentrations in the overlying water column (Jackson et al., 1998; Whiticar 2002; Treude et al., 2005; Bange et al., 2010). Results from monthly samplings during the last 10 years have revealed year-round methane seepage from the seafloor and methane supersaturation (with respect to the atmospheric equilibrium) of surface waters (Bange et al., 2010).
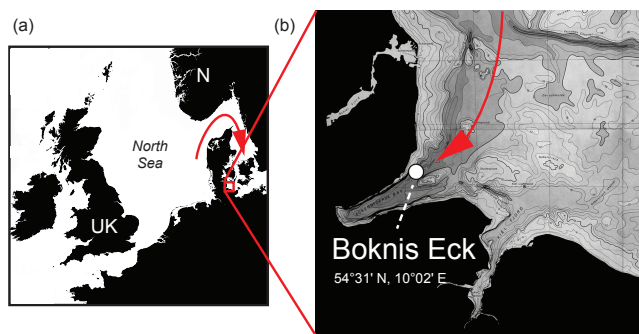
Figure 1. Map of the North Sea and the western Baltic Sea with a close-up of the study area. **(a)** Overview map of the western Baltic Sea including the Kattegat, the Skagerrak and parts of the North Sea. **(b)** Close-up of the study area with the sampling site (time-series station Boknis Eck) marked with a white dot. Red arrows indicate sporadic inflow of North Sea water.

The stratification period in Eckernförde Bay ends in autumn (October–November), with the onset of surface-water cooling and water-column mixing during autumn storms (Bange et al., 2010). Besides these seasonal water-column stability changes, episodic perturbations of the water column can be observed during occasional major saltwater injections from the North Sea. Such events occur over short time periods (days to weeks) when easterly winds are followed by strong westerly winds, leading to the inflow of salty, oxygen-enriched (autumn/winter) or oxygen-poor (summer) bottom water, respectively (Nausch et al., 2014; Mohrholz et al., 2015). As a result of variable exchange (not only during major saltwater injections) between North Sea and Baltic Sea water, bottom water salinity fluctuates strongly between 17 and 24 psu (Lennartz et al., 2014).

2.2 Sampling

Sampling was conducted every 3 months over a time period of 2 years (October 2012–September 2014). On board R/V *Alkor*, RC *Littorina* or RB *Polarfuchs*, water-column samples were collected from 1, 5, 10, 20, and 25 m below sea level (m b.s.l.) using a rosette sampler equipped with 6×4 L Niskin bottles and CTD (conductivity, temperature, depth) and O_2 probes for continuous measurements of conductivity, temperature, density, and dissolved oxygen, respectively (Hydro-Bios, Kiel, Germany; O_2-sensor: RINKO III). In the following, we use the common term CTD for the combined suite of sensors, including the O_2 sensor. We note that water column zones where the CTD oxygen sensor indicated $0 \, \mu mol \, L^{-1} \, O_2$ are not necessarily anoxic in the strict sense. Given that the detection limit of the Winkler method applied to calibrate the CTD oxygen sensor is $1–2 \, \mu mol \, L^{-1}$, micro-aerobic concentrations at the sub-μM levels were likely not detected as such. Water aliquots were sampled for measurements of methane concentration and MOx activity. For an

overview of sampling dates and corresponding parameters or incubations, see Table 1. In the following, samples from 1 and 5 m b.s.l. will be referred to as "surface waters", and samples from 20 and 25 m b.s.l. are considered "bottom waters".

2.3 Dissolved methane concentration

For dissolved methane (hereafter just methane) measurements, three 25 mL vials per sampling depth were filled bubble free immediately after CTD rosette recovery, poisoned with saturated mercury chloride solution ($50 \, \mu L$) and stored at room temperature. Methane concentrations were then determined by gas chromatography and flame ionization detection with a headspace method as described in Bange et al. (2010).

2.4 Methane oxidation rate measurements

MOx rates (r_{MOx}) were determined in quadruplicates from ex situ incubations of water samples with trace amounts of ^{3}H-labelled methane as described in Steinle et al. (2015) based on a previously described method (Reeburgh et al., 1991). In brief, 25 mL crimp-top vials were filled bubble free and closed with bromobutyl stoppers that are known to not affect MOx activity (Helvoet Pharma, Belgium; Niemann et al., 2015). Within a few hours after sampling, $6 \, \mu L$ of a gaseous ^{3}H-CH$_4$ / N$_2$ mixture (~ 15 kBq, < 30 pmol CH$_4$, American Radiolabeled Chemicals, USA) were added and samples were incubated for 3 days in the dark at in situ temperature ($\pm 0.5 \, ^\circ$C, Fig. 2c). The linearity of MOx during a time period up to 5 days was verified in selected samples by replicate incubations at 24, 48, 72, 96, and 120 h. At the end of the incubation, we determined the ^{3}H activities of the H$_2$O (A_{H_2O}; includes possible radio-label incorporation into biomass) and of non-reacted CH$_4$ (A_{CH_4}) by liquid scintillation counting. Activities were corrected for (insubstantial) fractional turnover ($\sim 0.1–0.01 \, \%$) in killed controls (addition of $100 \, \mu L$ saturated HgCl$_2$ solution). From these activities, we calculated the fractional turnover of methane (first-order rate constants; k; Eq. 1):

$$k = \frac{A_{H_2O}}{(A_{H_2O} + A_{CH_4})} \times \frac{1}{t}, \quad (1)$$

where t is incubation time.

r_{MOx} was then calculated from k and water column [CH$_4$] at the beginning of the incubation (see Sect. 2.4; Eq. 2):

$$r_{MOx} = k \times [CH_4]. \quad (2)$$

r_{MOx} from incubations with ^{14}C-labelled methane was determined analogously by measuring the radioactivity of ^{14}CH$_4$, ^{14}CO$_2$ (A_{CO_2}), and the remaining radioactivity (A_R), according to Blees et al. (2014) and Steinle et al. (2016). The use of ^{14}C also allows the assessment of methane incorporation
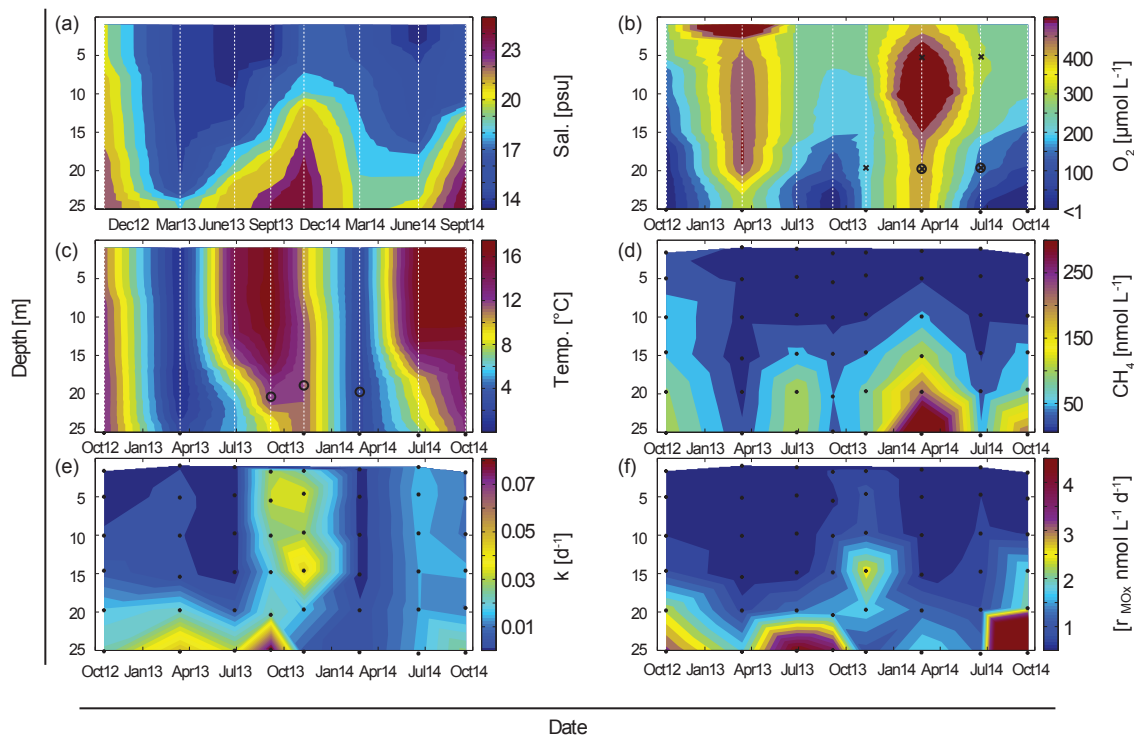
Figure 2. Seasonal variability of physico-chemical parameters and aerobic methanotrophy at the Boknis Eck station. Distribution of salinity **(a)**, oxygen **(b)**, temperature **(c)**, methane **(d)**, first-order rate constants of aerobic methane oxidation k **(e)**, and aerobic methane oxidation rates r_{MOx} **(f)**. Positions of discrete samples (dots) and continuous measurements (dashed lines) are indicated. Depths of water used for oxygen and temperature incubation experiments (Figs. 3 and 5) are indicated with circles in **(b)** and **(c)**. Depths of water used for biomass incorporation experiments at different oxygen concentrations (Figs. 4, S2) are indicated with crosses in **(b)**.

Table 1. Overview of sampling dates and sampled parameters. "Temp. dep." indicates samples used for temperature dependency incubations, "O_2 dep." indicates samples used for O_2 incubations with ^{3}H-CH$_4$ and ^{14}C-MOx for O_2 incubations with ^{14}C-CH$_4$ and determination of ^{14}C-incorporation into biomass.

| Sampling | Date | CH$_4$ | r_{MOx} | Temp. dep. | | O_2 dep. | | ^{14}C-MOx | |
				5 m b.s.l.	20 m b.s.l.	5 m b.s.l.	20 m b.s.l.	5 m b.s.l.	20 m b.s.l.
Oct 2012	17.10.2012	x	x						
Mar 2013	13.03.2013	x	x						
Jun 2013	27.06.2013	x	x						
Sep 2013	05.09.2013	x	x		x				
Nov 2013	08.11.2013	x	x	x	x		x[b]		x
Feb 2014	24.02.2014	x	x	x	x[a]	x	x[a]	x	x[a]
Jun 2014	18.06.2014	x	x	x	x	x	x	x	x
Sep 2014	17.09.2014	x	x	x	x				

[a] Because of disturbance of the water column, we used water from 25 m b.s.l. instead of 20 m b.s.l. [b] Because of disturbance of the water column, we used water from 15 m b.s.l. instead of 20 m b.s.l.

into biomass (Eq. 3):

$$C_{incorp.} = \frac{A_R}{A_{CO_2} + A_R}.$$ (3)

2.4.1 Oxygen manipulation experiments

Oxygen dependency experiments with the addition of ^{3}H-CH$_4$ were conducted with water from 25 m b.s.l. sampled in February 2014 (in situ concentrations of $[O_2] = 443 \, \mu mol \, L^{-1}$; $[CH_4] = 234 \, nmol \, L^{-1}$) and from 20 m b.s.l. in June 2014 (in situ concentrations of
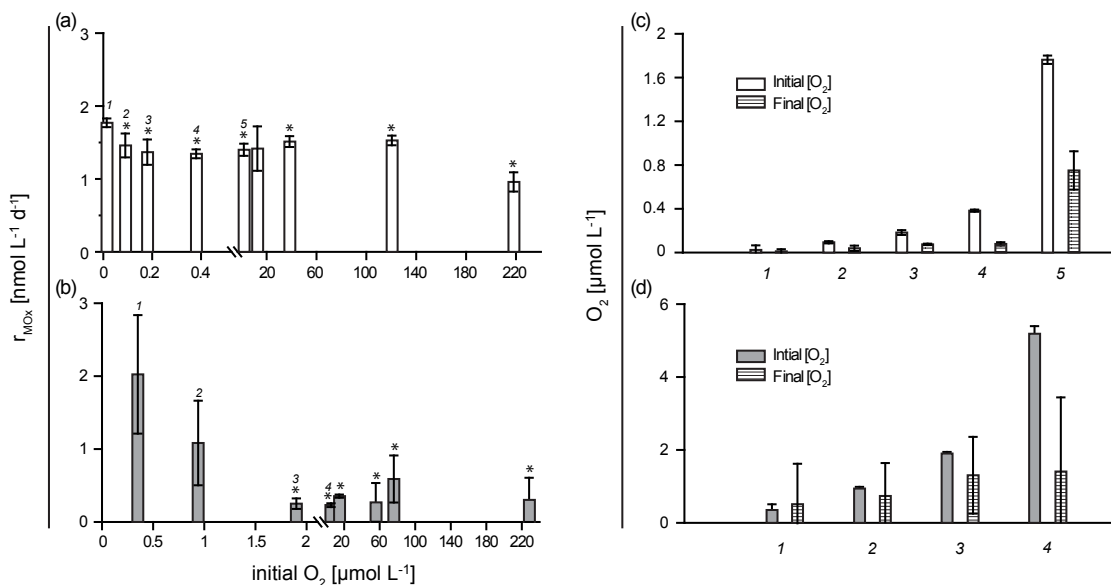
Figure 3. MOx rates in incubations with adjusted oxygen concentrations. r_{MOx} determined in incubations of Boknis Eck water (20 m b.s.l.) with ^{3}H-CH$_4$ in February 2014 **(a)** and June 2014 **(b)**. Asterisks indicate a $p < 0.05$ of a two-tailed, two-sample t test assuming equal variance of the MOx rate compared to the MOx rate of the lowest oxygen concentration. Corresponding oxygen concentrations determined at the beginning and the end of incubations from the February 2014 **(c)** and the June 2014 sampling **(d)** for incubations with oxygen concentration $< 10 \, \mu mol \, L^{-1}$. Numbers on the x axis of **(c)** and **(d)** correspond to numbers above the bars in **(a)** and **(b)** and indicate the incubation number. Incubations were performed in triplicates and standard deviations are indicated. For oxygen concentrations $> 10 \, \mu mol \, L^{-1}$, oxygen concentrations at the end of incubations were 14–40 % (February 2014) and 3–8 % (June 14) lower than at the beginning (data not shown).

$[O_2] = 161 \, \mu mol \, L^{-1}$; $[CH_4] = 34 \, nmol \, L^{-1}$). Until the start of the experiments (~ 5 days after sampling), the sampled water was stored headspace free at 0 °C. For the incubations, the water was filled into 160 mL glass vials, which were closed with gas-tight bromobutyl rubber stoppers (Helvoet Pharma, Niemann et al., 2015). Before use, the stoppers were boiled in water and stored under N$_2$ in order to avoid bleeding of oxygen from the rubber matrix into the vials. The vials were then purged for 30 min with high-purity N$_2$ gas, transferred to an anoxic glove box (N$_2$ atmosphere), and the N$_2$ headspace that was generated during the purging was exchanged with N$_2$-purged Boknis Eck water. For final oxygen concentrations $< 15 \, \mu mol \, L^{-1}$ (Fig. 3), we injected 0.1–8 mL of Boknis Eck water (in the glove box) that was previously equilibrated with ambient air. No additional oxygen was added to the incubation with the lowest oxygen concentration after purging the vials, resulting in oxygen concentrations $< 0.5 \, \mu mol \, L^{-1}$. For the final oxygen concentrations $> 15 \, \mu mol \, L^{-1}$, 10 ml headspace with a predefined gas mixture of O$_2$ / N$_2$ (5/95–12/88) was added, and the vials were left to equilibrate overnight at 4 °C. Additional vials were used to fill up the headspace the next day. After the oxygen adjustment, we added 12 µL of anoxic Boknis Eck water enriched in methane, resulting in a final methane concentration of $\sim 100 \, nmol \, L^{-1}$ in the incubation vial. For r_{MOx} determination, we added ^{3}H-CH$_4$ tracer in the glove box as described above. Oxygen concen-

tration was measured with a high-sensitivity (detection limit ca. 0.05 µM) OX-500 microsensor (Unisense). N$_2$-purged seawater amended with dithionite (final concentration 9 mmol L^{-1}) was used as a blank. Oxygen concentrations during incubations were determined by measuring initial and final oxygen concentration in parallel incubations, which were amended with 6 µL N$_2$ gas instead of ^{3}H-CH$_4$. Vials were incubated at 20 °C in the dark for 6 h ($[O_2] > 15 \, \mu mol \, l^{-1}$) or 10 h (for $[O_2] < 15 \, \mu mol \, L^{-1}$). In situ temperatures were 2.7 and 9.8 °C in February and June 2014, respectively. Incubation times differed because of time constraints during sample processing. r_{MOx} was determined as described above.

2.4.2 Incorporation of biomass at different oxygen concentrations

Incorporation of biomass at different oxygen concentrations was assessed using ^{14}C-CH$_4$ with water from 5 m b.s.l. sampled in February 2014 (in situ concentrations of $[O_2] = 581$; $[CH_4] = 22 \, nmol \, L^{-1}$) and June 2014 (in situ concentrations of $[O_2] = 301$; $[CH_4] = 14.5 \, nmol \, L^{-1}$), from 20 m b.s.l. sampled in November 2013 (in situ concentrations of $[O_2] = 234$; $[CH_4] = 82 \, nmol \, L^{-1}$) and June 2014 (in situ concentrations of $[O_2] = 161$; $[CH_4] = 34 \, nmol \, L^{-1}$), and from 25 m b.s.l. in February 2014 (in situ concentrations of $[O_2] = 443$; $[CH_4] = 234 \, nmol \, L^{-1}$; see also Table 1). Sam-

ples were prepared as described in Sect. 2.4.1 with the following modifications: we only performed the ^{14}C-CH$_4$ incubations with two different oxygen concentrations (<0.5 and $\sim 220\,\mu mol\,L^{-1}$), and used 220 mL instead of 160 mL glass vials. We added 10 μL of a ^{14}C-CH$_4$ / N$_2$ gas mixture ($\sim 200\,kBq$, $\sim 80\,\mu mol\,CH_4$, American Radiolabeled Chemicals, USA) to the samples. The vials were incubated for 6 h at 20 °C in the dark.

2.4.3 Temperature dependency experiments

Similar to the determination of r_{MOx} at in situ temperature, we incubated water column aliquots in triplicates at different temperatures between 0.5 and 37 °C in incubators. Exact temperatures are provided in Figs. 5 and S2. We determined the temperature dependency of MOx in samples collected at 5 and 20 m b.s.l. between September 2013 and September 2014 (Table 1). The MOx temperature optimum is defined here as the temperature where measured MOx rates were highest (i.e. not as the optimum for growth).

2.5 Areal MOx rates and methane release to the atmosphere

For each sampling date, we interpolated linearly between the measured rates at different depths, to obtain depth-integrated average rates for the 28 m-deep water column, and to calculate the methane oxidation rate per unit area (F_{MOx}; in μmol m^{-2} d^{-1}). Methane flux (F_{atm}; in μmol m^{-2} d^{-1}) from surface waters to the atmosphere was calculated according to Bange et al. (2010):

$$F_{atm} = k_{600} \times \left(Sc_{CH_4}/600\right)^{-0.5} \times \left([CH_4] - [CH_4]_{eq}\right), \quad (4)$$

where Sc_{CH_4} is the Schmidt number for CH$_4$, which is dependent on temperature and salinity, and is calculated as the ratio of kinematic viscosity of seawater (Siedler and Peters, 1986) and the diffusion coefficient of methane in seawater (Jähne et al., 1987). [CH$_4$] is the measured methane concentration at 1 m b.s.l., [CH$_4$]$_{eq}$ is the calculated CH$_4$ equilibrium concentration (Wiesenburg and Guinasso, 1979), with respect to average atmospheric pressure at sea level (measured at the Kiel Lighthouse, data available online on the website of the Federal Maritime and Hydrographic Agency of Germany; www.bsh.de) and the atmospheric methane concentration (median between 2012 and 2014) in the Northern Hemisphere (Mace Head Station; Prinn et al., 2014), and k_{600} is the gas transfer coefficient. Following the recommendation by Raymond and Cole (2001) for coastal systems, we used 3 and 7 cm h^{-1} as minimum and maximum values for k_{600}. These k_{600} values already include wind strength.

To determine the strength of water column stratification, we calculated the Brunt–Väisälä buoyancy frequency N:

$$N = \sqrt{-\frac{g}{\rho} \times \frac{d\rho}{dz}}, \quad (5)$$

where g is the gravitational constant, ρ is the potential density, and z is the geometric height. The average N (in cycles per hour; cph) was calculated for the depth interval 10–20 m b.s.l.

2.6 Statistical analyses

The pairwise linear correlations of different physico-chemical factors with methane concentrations and MOx rate constants and MOx rates were calculated in Matlab with the corr(X,Y, "Pearson", "both") function to obtain the Pearson linear correlation coefficient and the corresponding p value. In the results and discussion section, all presented R^2 values are Persons linear correlation coefficients.

3 Results

3.1 Seasonal variations of physico-chemical water column properties

Physico-chemical water column properties generally showed large seasonal variations (Fig. 2). Salinity varied strongly in bottom (18–25 psu) and surface waters (13–20 psu) with the highest salinities observed in September–November (Fig. 2a). During winter samplings, water temperatures were coldest and rather invariant throughout the water column at 1–3 °C (March 2013, February 2014; Fig. 2b). They increased from spring until the end of summer to a maximum of 18 °C in the surface (June 2013, September 2014) and 13 °C in bottom waters (October 2012, September 2014). Dissolved oxygen concentrations in bottom waters varied from <1 to $450\,\mu mol\,L^{-1}$ (Fig. 2c), with the highest concentrations observed during fully mixed conditions (March 2013, February 2014). In March 2013 and February 2013, chlorophyll a concentrations were comparably high (data not shown, available at www.bokniseck.de), indicating a phytoplankton bloom during these time periods. Bottom waters became hypoxic in June (2013, 2014) and reached oxygen concentrations $\leq 1\,\mu mol\,L^{-1}$ towards the end of the stratification period (September 2013, 2014). In surface waters, levels of dissolved oxygen were always high ($>280\,\mu mol\,L^{-1}$), reaching maximum concentrations during a phytoplankton bloom in March 2013 and February 2014 ($>450\,\mu mol\,L^{-1}$; Fig. 2c). Dissolved methane concentrations reached values up to $466 \pm 13\,nmol\,L^{-1}$ (March 2014) in bottom waters, and were always $>30\,nmol\,L^{-1}$ during the time of our study (Fig. 2d). We did not observe a clear repeating seasonal pattern of methane concentrations in the 2 years of our study. Surface-dissolved methane concentrations ranged between 8 and 27 nmol L^{-1}, corresponding to supersaturation levels of 270–870 % with respect to the atmospheric equilibrium (2.8–4.3 nmol L^{-1}).

3.2 Seasonal variability of MOx

First-order rate constants (k) of MOx were always highest in bottom waters (0.003–$0.084\,\mathrm{d}^{-1}$) with the exception of November 2013 when the highest k was measured at 15 m b.s.l. (Figs. 2e, S1 in the Supplement). The same pattern was found for r_{MOx}, which was always highest in bottom waters (1.0–$11.6\,\mathrm{nmol\,L}^{-1}\,\mathrm{d}^{-1}$), again with the exception of November 2013 (Fig. 2f). The highest values for r_{MOx} were observed in summer (June 2013) or autumn (October 2012, September 2013, September 2014) when bottom water temperatures were highest and oxygen concentration were lowest. A correspondence between maximum r_{MOx} and high/maximum CH_4 concentrations (i.e. in March 2014) was not observed.

3.3 Experiments on the influence of oxygen concentrations on MOx activity

In the subsequent presentation of experimental data, hypoxic conditions (i.e. $[O_2] < 63\,\mathrm{\mu mol\,L}^{-1}$) will be referred to as "low" and $[O_2] > 63\,\mathrm{\mu mol\,L}^{-1}$ as "high" oxygen concentrations for the sake of simplicity. During our lab-based experiments with different oxygen concentrations, r_{MOx} was always highest in incubations with the lowest oxygen concentration (Tables S1, S2 in the Supplement, Fig. 3). Rates under nearly saturated oxygen conditions were significantly lower (50 % in February, 75 % in June; $p < 0.05$) than the rate measured at the lowest initial oxygen concentration. However, while we found that r_{MOx} did not vary strongly at different oxygen concentrations $< 140\,\mathrm{\mu mol\,L}^{-1}$ (Fig. 3a) in February 2014, the rates measured in June 2014 were more variable (Fig. 3b).

All incubations remained oxic during the incubation time, even incubations with very low initial oxygen concentrations (Tables S1, S2, Fig. 3c, d). In February 2014, 41–79 % of oxygen was consumed during incubations with initial $[O_2]$ $< 15\,\mathrm{\mu mol\,L}^{-1}$ (Fig. 3c), and 14–40 % during incubations with initial $[O_2] > 15\,\mathrm{\mu mol\,L}^{-1}$ (Table S1). In June 2014, 22–73 % of the oxygen was consumed during incubations with initial $[O_2] < 15\,\mathrm{\mu mol\,L}^{-1}$ (Fig. 3d), and 3–8 % during incubations with $[O_2] > 15\,\mathrm{\mu mol\,L}^{-1}$ (Table S2).

Similar to incubations with ^{3}H-CH_4, k values determined with ^{14}C-CH_4 at saturated oxygen concentration were lower than k values measured in incubations with $[O_2] < 0.5\,\mathrm{\mu mol\,L}^{-1}$ (32 % lower on average; Figs. 4a, S2a, b). In contrast, a higher fraction of the oxidized ^{14}C was incorporated into biomass in incubations at saturated oxygen concentration than at $[O_2] < 0.5\,\mathrm{\mu mol\,L}^{-1}$ (between 108 and 3800 % more; Figs. 4b, S2c, d), irrespective of water depth and sampling season (Fig. S2). Radio-label incorporation at low oxygen levels ($[O_2] < 0.5\,\mathrm{\mu mol\,L}^{-1}$) was generally more pronounced in bottom (20 m b.s.l.) than in surface waters (5 m b.s.l.).

3.4 Temperature dependence of MOx

In general, k increased with temperature and reached maximum values at 20–37 °C, indicating a mesophilic temperature optimum (Fig. 5a, c; shown are results from September 2013 and February 2014; Table 1; Fig. S3). Only in November 2013, maximum MOx was observed at 10–20 °C, consistent with a psychrophilic temperature optimum (Fig. 5b). These patterns were independent of water depth (Figs. 5, S3).

3.5 Water-column methane removal by MOx and methane fluxes to the atmosphere

Depth-integrated r_{MOx} ($= F_{\mathrm{MOx}}$) varied between $11.7\,\mathrm{\mu mol\,m}^{-2}\,\mathrm{d}^{-1}$ (March 2013) and $82.3\,\mathrm{\mu mol\,m}^{-2}\,\mathrm{d}^{-1}$ (September 2014; Table 2). Estimated average fluxes of methane to the atmosphere were 3.6–$9.2\,\mathrm{\mu mol\,m}^{-2}\,\mathrm{d}^{-1}$ during stratified periods, and 10.0–$25.1\,\mathrm{\mu mol\,m}^{-2}\,\mathrm{d}^{-1}$ during mixed periods (considering a minimum or maximum k_{w}, respectively; Table 2; Raymond and Cole 2001). According to the buoyancy frequency N, we grouped the sampling dates into two categories: weakly (i.e. $N < 120$ cph) and strongly stratified (i.e. $N > 120$ cph). The water column was only weakly stratified in October 2012, March 2013, and February 2014, and strongly stratified during all other samplings (Table 2).

4 Discussion

4.1 Seasonal variations at Boknis Eck

4.1.1 Development of seasonal hypoxia

Oxygen concentrations were always close to saturation levels during our winter samplings (i.e. March 2013, February 2014), when the water column was poorly stratified and phytoplankton blooms occurred, which is typical for this time period (Bange et al., 2010). During June samplings, we observed much lower bottom water oxygen concentrations, indicating the onset of hypoxia, reaching submicromolar oxygen concentrations below 24 m b.s.l. in September (2013, 2014). Our observation is in accordance with a previous time series study (2006–2008) by Bange et al. (2010), who found hypoxic events starting between May and August and lasting until September or November. Long-term monitoring at Boknis Eck showed that the frequency and length of hypoxic events have increased over the last 20 years (Lennartz et al., 2014), although nutrient inputs into the Baltic Sea were strongly reduced (HELCOM, 2009). One of the main reasons for the ongoing decrease in oxygen concentration is the increasing water temperature since the 1960s (Lennartz et al., 2014). Higher surface water temperatures have led to an extension of the stratification period (starting earlier in the annual cycle), reducing the overall exchange between bottom and surface waters (Hoppe et al., 2013; Lennartz et al., 2014).
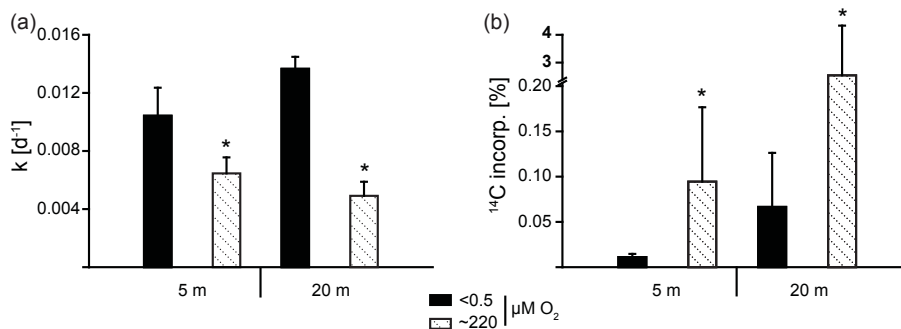
Figure 4. Methane–carbon assimilation in relation to oxygen concentration. Methane–carbon assimilation was determined from incubations amended with ^{14}C-CH$_4$ at saturated ($\sim 220\,\mu\mathrm{mol\,L^{-1}}$, shaded bars) or low oxygen concentrations ($< 0.5\,\mu\mathrm{mol\,L^{-1}}$, black bars) of water recovered in June 2014 at 5 and 20 m b.s.l. Incubations were performed in triplicates and standard deviations are indicated. **(a)** First-order rate constant (k). **(b)** Fraction of oxidized methane incorporated into biomass. Asterisks indicate a p value < 0.05 of a two-tailed, two-sample t test assuming equal variance between the samples at low and high oxygen concentrations.
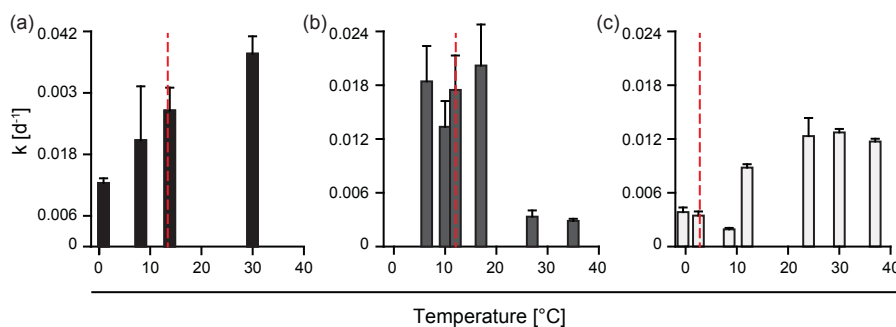
Figure 5. MOx first-order rate constants (k) at different temperatures. First-order rate constants of MOx were determined with ^{3}H-CH$_4$ amendments in triplicated incubations of water from 20 m b.s.l. recovered in September 2013 **(a)**, November 2013 **(b)**, and February 2014 **(c)**. Red, dashed lines indicate in situ temperatures.

Furthermore, a general increase in temperature also enhances mineralization of organic matter in bottom waters and results in a higher biological oxygen demand (Hoppe et al., 2013; Lennartz et al., 2014).

4.1.2 Seasonal dynamics of methane concentrations and MOx

Methane concentrations at Boknis Eck were in a similar range to other shelf seas and coastal ecosystems (e.g. Rehder et al., 1998; Bange, 2006; Upstill–Goddard 2016). We did not observe any clear seasonal methane concentration patterns as observed for oxygen concentrations and other physico-chemical parameters (Fig. 2). Our data are consistent with observations from 2006 to 2008 by Bange et al. (2010), who showed that methane concentrations did not follow bi-modal seasonal variations. Instead, increases in water col-umn methane followed chlorophyll a concentrations in sur-face waters with a 1-month time lag, suggesting that pulses of elevated organic matter input to the sediments were boosting benthic methanogenesis.

We did not observe direct links between water col-umn oxygenation and methane concentrations ($R^2 = 0.007$; $p = 0.6$). However, water column oxygen concentrations can have indirect and inverse effects on methane concentra-tions: low oxygen concentrations combined with high sed-imentation rates of organic matter lead to enhanced burial of "fresh" organic matter to the sediments, which in turn favours methanogenesis at Boknis Eck (Bange et al., 2010; Maltby, 2015). Furthermore, water column stratification at times of water column hypoxia at Boknis Eck hinders ex-change between bottom and surface waters, which further promotes methane accumulation in bottom waters. Such a modulating effect of oxygen on methane concentrations has also been found in other hypoxic ecosystems (see review by Naqvi et al., 2010). Nonetheless, the highest methane con-centrations were not always observed during periods of min-imum oxygen concentrations. On the contrary, we found re-duced net methane accumulation in bottom waters at times of hypoxia and strong water column stratification (sum-mer/autumn 2013, Fig. 2), likely caused by the comparatively high MOx rates observed during this time period.

Table 2. Integrated methane oxidation rates (F_{MOx}) and methane flux into the atmosphere (F_{atm}) in comparison to stratification (indicated by the buoyancy frequency N). F_{atm} was calculated with a min and max k_{600}-value. N is given as the average N for 10–20 m b.s.l. A water column with N values > 120 is considered stratified.

Sampling	F_{MOx} ($\mu mol\,m^{-2}\,d^{-1}$)	$F_{atm} - min\,k_{600}$ ($\mu mol\,m^{-2}\,d^{-1}$)	$F_{atm} - max\,k_{600}$ ($\mu mol\,m^{-2}\,d^{-1}$)	F_{MOx}/F_{atm}	N (cph)
Oct 2012	29.6	12.4	31.1	1.4	87
Mar 2013	11.7	10.5	26.4	0.6	66
Jun 2013	27.3	3.2	7.9	4.9	247
Sep 2013	33.0	3.4	8.5	5.6	229
Nov 2013	28.0	6.3	15.8	2.5	211
Feb 2014	14.5	7.0	17.6	1.2	114
Jun 2014	12.7	2.9	7.4	2.4	200
Sep 2014	82.3	2.5	6.2	19.0	227

We did not observe a direct stimulus of high methane concentrations on the turnover rate constant k ($R^2 = 0.1$; $p = 0.6$). For example, we found low methane concentrations in March 2013 co-occurring with high turnover constants, while high methane concentrations in September 2014 were also accompanied by elevated turnover constants. Previous studies suggested an inverse relationship between turnover time (i.e. $1/k$) and methane concentrations (Elliott et al., 2011; Nauw et al., 2015; Osudar et al., 2015; James et al., 2016). Although this relationship may be robust across different environmental settings, several studies found that on a smaller, local scale the CH_4/k connection does not necessarily apply (Heintz et al., 2012; Mau et al., 2012; Steinle et al., 2015, 2016).

MOx rates at Boknis Eck were of the same order of magnitude as those measured in other coastal environments (e.g. Abril and Iversen 2002; Mau et al., 2013; Osudar et al., 2015). MOx measurements in this study revealed seasonal dynamics, with lower rates during the winter season when the water column was mixed and oxygen concentrations were high (March 2013, February 2014), and highest rates during stratified, hypoxic conditions (June–October). Our data suggest a negative dependency of r_{MOx} with oxygen concentration ($R^2 = 0.49$; $p = 0.001$), whereas this was not the case with temperature ($R^2 = 0.03$; $p = 0.82$). In order to further investigate these putative links observed during the time-series study, we conducted laboratory experiments to specifically assess the effects of oxygen concentration (Sect. 4.2) and temperature (Sect. 4.3) on MOx.

4.2 Aerobic methanotrophy under micro-oxic conditions

We observed the highest MOx rates in September 2013 and September 2014 (Fig. 2f), when bottom water oxygen concentrations were below the detection limit of the oxygen sensor (i.e. 1–2 $\mu mol\,L^{-1}$). Whether oxygen concentrations reached true zero levels is unclear. Our measurements did not reveal hydrogen sulfide concentrations in the water column, and the absence of any hydrogen sulfide smell points to the fact that traces of oxygen were probably still present. Anaerobic oxidation of methane (AOM) thus seems unlikely to account for the observed oxidation rates since anaerobic methanotrophs cannot persist in the presence of oxygen even at submicromolar levels (Treude et al., 2005; Knittel and Boetius, 2009). Other recent studies in lakes reported on the occurrence of aerobic methanotrophy in apparently anoxic environments (Blees et al., 2014; Milucka et al., 2015; Oswald et al., 2015). Two of these studies showed that, in the presence of light, photosynthetic algae create oxic microniches and provide enough oxygen for MOx to proceed under otherwise anoxic conditions (Milucka et al., 2015; Oswald et al., 2015). We cannot rule out that in situ MOx in oxygen-depleted waters of Boknis Eck was, at least to some degree, fuelled by photosynthesis in bottom waters. However, light intensities deeper than 20 m b.s.l. in the murky waters at Boknis Eck are likely too low to account for the observed high rates. Furthermore, in the dark-incubation experiments of this study, rates were still highest at the lowest oxygen concentration (Tables S1, S2, Fig. 3), arguing against any significant photosynthetic production of oxygen to support light-dependent MOx. In another lake study, a large potentially active MOx community was discovered in the anoxic hypolimnion > 125 m below the lake surface, where light-dependent MOx can be excluded (Blees et al., 2014). It was hypothesized that sporadic oxygen inflow was sufficient to sustain a viable MOx community in anoxic waters, well below the permanent redoxcline. At Boknis Eck, it is possible that episodic oxygen inputs through horizontal advection can occur, as has been observed after North Sea water inflows into the anoxic basins of a Danish fjord (Zopfi et al., 2001) and the Baltic Sea (Schmale et al., 2016). Although we cannot say without doubt what the sources of oxygen are that sustain MOx under micro-oxic conditions our incubation experiments with oxygen concentrations as low as $\sim 0.1\,\mu mol\,L^{-1}$ show that MOx rates remain high at such low concentration (Figs. 3, 4). This consequently provides evidence that MOB are well adapted to the seasonally sub-

micromolar oxygen levels in bottom waters at Boknis Eck, Baltic Sea.

Whereas plausible explanations exist for the presence and activity of MOB under seemingly oxygen-starved conditions, we still lack an explanation for the observation that in our incubations MOx rates were highest at the lowest oxygen levels, independently of the initial oxygenation state of the sampled water (Fig. 3). The apparent adaptation to low oxygen concentrations may be part of a strategy to avoid the detrimental effects of methane starvation under oxic conditions and to escape grazing pressure in more oxygenated water. For example, grazers were found to control the community size of MOB in shallow Finnish lakes (Devlin et al., 2015). The ability of MOB to operate at low oxygen levels apparently enables them to thrive in bottom waters with only trace amounts of oxygen. Additionally, reduced grazing activity under hypoxia may allow efficient MOB community growth, which would lead to elevated MOx activity in these water layers. Indeed, direct links between the MOB community size and MOx have been demonstrated before (e.g. Steinle et al., 2015). We did not investigate zooplankton in our ex situ incubations, and hence, do not know whether limited grazing within the incubations themselves at low oxygen levels was responsible for the observed trend of highest MOx rates at low oxygen levels.

Enhancement of MOx rates in incubations at low oxygen levels can also be explained at the cellular/biochemical level. Aerobic microbes produce reactive oxygen species (ROS; including superoxide anion radicals, hydrogen peroxide, and hydroxyl radicals) as by-products during their metabolism, which can cause oxidative damage to cellular structures. The amount of ROS leaking from the respiratory chain typically increases at elevated oxygen concentrations (see review by Baez and Shiloach, 2014). Although we can only speculate as to how effectively MOB are able to remove ROS (e.g. by catalase), it seems possible that MOx may be slowed down at high oxygen concentrations. However, the fraction of ^{14}C incorporated into biomass was markedly higher at elevated oxygen concentration, even though MOx rates were higher at low oxygen concentration (Fig. 4), which rather suggests differential metabolic functioning of MOB at low versus high oxygen concentrations. Kalyuzhnaya et al. (2013) showed that, under oxygen-deficiency stress ($< 10\,\mu mol\,L^{-1}$), a strain of type I MOB (*Methylomicrobium alcaliphylum* 20Z) switched to fermentative methane utilization, leading to a reduced MOB-biomass synthesis and the enhanced formation of short-chain carbonic acids (i.e. formate, acetate, succinate) as metabolic end products. If the Boknis Eck-MOB employed a similar, energetically less favourable methane utilization pathway, our results could be explained by an overall higher catabolic activity at the cost of anabolic investment at low oxygen concentrations. Additional biochemical investigations are necessary to constrain the metabolic partitioning of MOB at high versus low oxygen levels further, but also to test the potential role of ROS in MOx attenuation at elevated oxygen levels. Finally, we cannot rule out that MOx in our incubations (and at Boknis Eck) is mediated by a diverse MOB community, of which different members are active at different oxygen levels. Such a shift may also lead to the observed discrepancies in the MOx rate and metabolic functioning.

4.3 Temperature effects on MOx

4.3.1 Mesophilic behaviour of MOx and implications for future warming

With the exception of November 2013 (see Sect. 4.4, below), the MOB community at Boknis Eck generally showed a mesophilic behaviour, with temperature optima > 10 and $< 37\,°C$, both in bottom (Fig. 5) and surface waters, respectively (Fig. S3). This is consistent with temperature optimum ranges observed for most cultured aerobic methanotrophs (Hanson and Hanson, 1996; Murrell, 2010). Except for November 2013 (see Sect. 4.3.2), the temperature optimum was ~ 5–$20\,°C$ higher than the in situ temperature (at the time of sampling), which is typical for many microorganisms (Price and Sowers 2004). The ongoing increase in atmospheric temperature has led to a global sea surface temperature anomaly of about $0.5\,°C$ (until 2010), and future projections indicate further warming by up to $2\,°C$ until the middle of the 21st century (IPCC, 2013). A similar warming trend is observed for the Baltic Sea (HELCOM, 2009). It is unclear how exactly surface water warming (and associated physico-biogeochemical side effects in the upper water column) will influence bottom water temperatures in the future. Particularly in shallow shelf seas, however, ocean surface warming is likely to propagate to deeper water layers, and indeed, such a warming trend has been recorded at Boknis Eck (Lennartz et al., 2014). Our incubation experiments indicate that the present MOB community is well adapted to temperature changes of a few degrees Celsius, and that r_{MOx} will probably increase in the near future.

4.3.2 Indirect evidence for a change of the MOB community by North Sea water inflow events

Contrary to the general mesophilic MOB community at Boknis Eck, incubations with water samples from November 2013 (Figs. 5b, S3a) revealed a psychrophilic behaviour of the MOB with a much lower temperature optimum at about $10\,°C$. In November 2013, in situ temperatures were 12.0 and $10.6\,°C$ at 20 and $5\,m$ b.s.l., respectively. In contrast to all other sampling dates, the temperature optimum hence corresponded to the in situ temperature. These differences suggest the presence of another microbial MOB community at Boknis Eck in November 2013 compared to the other sampling times. The sampling took place on 8 November 2013, about 1 week after a larger inflow event that transported oxygen-rich, salty North Sea water into the Baltic Sea. This input

is clearly indicated by salinity anomalies observed at several hydrographic measurement stations of the Federal Maritime and Hydrographic Agency of Germany (Nausch et al., 2014), including the nearby station, Kiel Lighthouse. No continuous salinity measurements were conducted at Boknis Eck to provide evidence for the saltwater injection directly at the study site. However, the unusual oxygen profile with a distinct minimum at 15 m b.s.l. and increasing oxygen concentrations in bottom waters seems to attest to the October inflow event, during which dense undercurrents of salt- and oxygen-rich water from the North Sea were wedging into, and (partly) displacing, the hypoxic deep Eckernförde Bay water (Fig. S1).

In November 2013, maximum k and r_{MOx} were detected at 15 m b.s.l., and not in bottom waters, as it was the case during all the other samplings (Figs. 2, S1). In combination with the observed shift from a meso- to a psychrophilic community, this suggests that with the inflowing North Sea water, the local MOB community at Boknis Eck was displaced. North Sea water is characterized by elevated methane concentrations (Rehder et al., 1998) and relatively high water column MOx rates were detected at several sites in the North Sea (Mau et al., 2015; Osudar et al., 2015; Steinle et al., 2016), so that the inflowing water may indeed contain relatively high numbers of MOB. However, the inflow and the transient replacement of hypoxic Eckernförde Bay water (including its microbial stock) has led to reduced MOx rates by the imported psychrophilic compared to the autochthonous mesophilic MOB community near the sea floor. Similarly, current-associated translocation of MOx communities has been found to constitute an important control on the magnitude of local MOx rates offshore Svalbard (Steinle et al., 2015). In Eckernförde Bay, further studies that include molecular work would be needed to investigate the origin of the seemingly differential MOB communities, their actual cell numbers, and the effects of sporadic, short-term perturbations on the MOx potential.

4.4 Considerable methane removal by MOx

The median methane efflux into the atmosphere calculated from our measurements (5.1 or 11.9 μmol m^{-2} d^{-1}, considering min. and max. values for k, respectively) was very similar to previous data from a monthly sampling campaign at Boknis Eck between 2006 and 2008 (6.3–14.7 μmol m^{-2} d^{-1}; Bange et al., 2010). Average surface saturation (447 % with respect to atmospheric equilibrium) at Boknis Eck was at the lower end of European estuarine systems and river plumes, but clearly higher than values determined for European shelf waters (Upstill-Goddard et al., 2000; Bange, 2006; Schubert et al., 2006; Grunwald et al., 2009; Ferrón et al., 2010; Schmale et al., 2010; Osudar et al., 2015; Upstill-Goddard and Barnes, 2016). At Boknis Eck, methane originates from sedimentary methanogenesis (Whiticar 2002; Treude et al., 2005; Maltby, 2015), which can enter the water column either by diffusion or by bubble transport. The amplitudes of

methanogenesis and AOM were found to show strong spatio-temporal heterogeneity, which makes flux estimates difficult (Treude et al., 2005; Maltby, 2015). However, our data allow calculating the amount of water column methane oxidation compared to the fraction of methane that ultimately evades to the atmosphere (i.e. $F_{\mathrm{MOx}} / F_{\mathrm{atm\text{-}avg}}$; possible effects of advection on methane concentration and MOx are ignored). Our depth-integrated MOx rates and the average of our minimum and maximum estimates of methane efflux to the atmosphere imply that 2.4–19 times more methane is oxidized than is emitted to the atmosphere during stratified conditions (Table 2), underscoring the high efficiency of the water column methane filter during summer/autumn, albeit the shallow water depth. In contrast, almost the same amount of methane is oxidized and emitted (factor of 0.6–1.4) during mixed conditions in winter/spring. This difference is mostly due to the lower average F_{atm} under stratified conditions, as F_{atm} correlates negatively with buoyancy frequency ($R^2 = 0.8$; Fig. S4). However, F_{MOx} was also highest in autumn months (September–November), and lowest in winter/spring (February–March; Table 2). Under stratified conditions, the combination of a generally higher (community-driven) MOx potential and the limited exchange between bottom waters and the upper mixed layer, and hence a lower turbulent diffusive methane flux, are conducive to efficient methane oxidation and contribute to the higher MOx filter capacity during summer/autumn. In conclusion, seasonal water column stratification and, consequently, lower oxygen concentrations thus not only promote generally higher rates of MOx but also have a modulating effect on the efficiency of the microbial methane filter in the water column.

5 Conclusions and implications

To the best of our knowledge, this is the first long-term (> 2 years) seasonal study on MOx activity in a seasonally stratified/hypoxic coastal environment. The results are important for the understanding of the temporal dynamics and environmental controls on the efficiency of the MOx methane filter in shallow marine environments. We demonstrate that methane oxidation at Boknis Eck is strongly affected by changes of water column stratification, as well as by inflow events from the North Sea, and the associated episodic displacement of bacterial communities with different MOx potential. Moreover, we provide evidence that MOB at Boknis Eck are well adapted to very low oxygen concentrations, with a clear tendency of the highest MOx rates occurring in the submicromolar range. Although the exact ecological driving forces, as well as the biochemical mechanisms behind this adaptation remain uncertain, it seems likely that the capacity to thrive in low-oxic waters enables MOB to evade grazing pressure in the more oxygenated parts of the water column.

Our field and laboratory investigations revealed that very low oxygen concentrations under stratified conditions and

at elevated temperatures are particularly conducive to high MOx rates and efficient methane "removal" from the water column. Ongoing trends at Boknis Eck (and in many other coastal ecosystems) predict warmer temperatures in the future, and probably an earlier onset of seasonal stratification. However, for a future scenario, it remains unclear as to what extent the low-oxygen adaptation and a temperature-related enhancement of MOx will counterbalance elevated rates of methanogenesis in the sediments caused by higher temperatures. Our study suggests that an extension of the hypoxic period and increasing temperatures will not necessarily lead to higher methane evasion to the atmosphere. Ultimately, the oxygen–MOx link will also depend on the potential inhibition of MOB growth under oxygen-depleted conditions. Our experimental data suggest that the MOB communities can experience growth restrictions under oxygen-deficiency stress, but whether the expected spatio-temporal expansion of hypoxia, and eventually anoxia, may finally hamper MOx has to be investigated further.

Data availability. All data presented in this paper are available in the PANGAEA data repository (doi:10.1594/PANGAEA.871890, Steinle et al., 2017).

The Supplement related to this article is available online at doi:10.5194/bg-14-1631-2017-supplement.

References

Abril, G. and Iversen, N.: Methane dynamics in a shallow non-tidal estuary (Randers Fjord, Denmark), March Ecol.-Prog. Ser., 230, 171–181, 2002.

Baez, A. and Shiloach, J.: Effect of elevated oxygen concentration on bacteria, yeasts, and cells propagated for production of biological compounds, Microb. Cell Fact., 13, p. 181, 2014.

Bakker, D. C., Bange, H. W., Gruber, N., Johannessen, T., Upstill-Goddard, R. C., Borges, A. V., Delille, B., Löscher, C. R., Naqvi, S. W. A., Omar, A. M., and Santana-Casiano, J. M.: Air–sea interactions of natural long-lived greenhouse gases (CO$_2$, N$_2$O, CH$_4$) in a changing climate, in: Ocean-Atmosphere Interactions of Gases and Particles, edited by: Liss, P. S. and Johnson, M. T., Springer Verlag, 113–169, 2014.

Bange, H. W: Nitrous oxide and methane in European coastal waters, Estuar. Coast. Shelf S., 70, 361–374, 2006.

Bange, H. W., Bartell, U. H., Rapsomanikis, S., and Andreae, M. O.: Methane in the Baltic and North Seas and a reassessment of the marine emissions of methane, Global Biogeochem. Cy., 8, 465–480, 1994.

Bange, H. W., Bergmann, K., Hansen, H. P., Kock, A., Koppe, R., Malien, F., and Ostrau, C.: Dissolved methane during hypoxic events at the Boknis Eck time series station (Eckernförde Bay, SW Baltic Sea), Biogeosciences, 7, 1279–1284, doi:10.5194/bg-7-1279-2010, 2010.

Bange, H. W., Hansen, H. P., Malien, F., Laß, K., Dale, A. W., Karstensen, J., Petereit, C., and Friedrichs, G.: Boknis Eck time series station (SW Baltic Sea): measurements from 1957 to 2010, LOICZ inprint, 1, 16–22, 2011.

Blees, J., Niemann, H., Wenk, C.B., Zopfi, J., Schubert, C.J., Kirf, M.K., Veronesi, M. L., Hitz, C., and Lehmann, M. F.: Micro-aerobic bacterial methane oxidation in the chemocline and anoxic water column of deep south-Alpine Lake Lugano (Switzerland), Limnol. Oceanogr., 59, 311–324, 2014.

Boetius, A. and Wenzhöfer, F.: Seafloor oxygen consumption fuelled by methane from cold seeps, Nat. Geosci., 6, 725–734, 2013.

Bussmann, I. and Suess, E.: Groundwater seepage in Eckernförde Bay (Western Baltic Sea): Effect on methane and salinity distribution of the water column, Cont. Shelf Res., 18, 1795–1806, 1998.

Canfield, D. E. and Thamdrup, B.: Towards a consistent classification scheme for geochemical environments, or, why we wish the term suboxic would go away, Geobiology, 7, 385–392, 2009.

Carini, S., Bano, N., LeCleir, G., and Joye, S. B.: Aerobic methane oxidation and methanotroph community composition during seasonal stratification in Mono Lake, California (USA), Environ. Microbiol., 7, 1127–1138, 2005.

Devlin, S. P., Saarenheimo, J., Syväranta, J., and Jones, R. I.: Top consumer abundance influences lake methane efflux, Nat. Commun., 6, p. 8787, 2015.

Diaz, R. J. and Rosenberg, R.: Spreading dead zones and consequences for marine ecosystems, Science, 321, 926–929, 2008.

Elliott, S., Maltrud, M., Reagan, M., Moridis, G., and Cameron–Smith, P.: Marine methane cycle simulations for the period of early global warming, J. Geophys. Res.-Biogeo., 116, G01010, doi:10.1029/2010JG001300, 2011.

Ferrón, S., Ortega, T., and Forja, J. M.: Temporal and spatial variability of methane in the north-eastern shelf of the Gulf of Cádiz (SW Iberian Peninsula), J. Sea R., 64, 213–223, 2010.

Ferry, J. G. (Ed.): Methanogenesis. New York, Chapman and Hall, 1993.

Friedrich, J., Janssen, F., Aleynik, D., Bange, H. W., Boltacheva, N., Çagatay, M. N., Dale, A. W., Etiope, G., Erdem, Z., Geraga, M., Gilli, A., Gomoiu, M. T., Hall, P. O. J., Hansson, D., He, Y., Holtappels, M., Kirf, M. K., Kononets, M., Konovalov, S., Lichtschlag, A., Livingstone, D. M., Marinaro, G., Mazlumyan, S., Naeher, S., North, R. P., Papatheodorou, G., Pfannkuche, O., Prien, R., Rehder, G., Schubert, C. J., Soltwedel, T., Sommer, S., Stahl, H., Stanev, E. V., Teaca, A., Tengberg, A., Waldmann, C., Wehrli, B., and Wenzhöfer, F.: Investigating hypoxia in aquatic environments: diverse approaches to addressing a complex phenomenon, Biogeosciences, 11, 1215–1259, doi:10.5194/bg-11-1215-2014, 2014.

Gelesh, L., Marshall, K., Boicourt, W., and Lapham, L.: Methane concentrations increase in bottom waters during summertime anoxia in the highly eutrophic estuary, Chesapeake Bay, USA, Limnol. Oceanogr., 61, S253–S266, doi:10.1002/lno.10272, 2016.

Grunwald, M., Dellwig, O., Beck, M., Dippner, J. W., Freund, J. A., Kohlmeier, C., Schnetger, B., and Brumsack, H.-J.: Methane in the southern North Sea: Sources, spatial distribution and budgets, Estuar. Coast. Shelf S., 81, 445–456, 2009.

Hansen, H. P., Giesenhagen, H. C., and Behrends, G.: Seasonal and long-term control of bottom-water oxygen deficiency in a stratified shallow-water coastal system, ICES J. March Sci., 56, 65–71, 1999.

Hanson, R. S. and Hanson, T. E.: Methanotrophic bacteria, Microbiol. Rev., 60, 439–471, 1996

Heintz, M. B., Mau, S., and Valentine, D. L.: Physical control on methanotrophic potential in waters of the Santa Monica Basin, Southern California, Limnol. Oceanogr., 57, 420–432, 2012.

HELCOM: Eutrophication in the Baltic Sea – an integrated assessment of the effects of nutrient enrichment in the Baltic Sea region, Baltic Sea Environ. Proc., 115, 1–145, 2009.

Hoppe, H.-G., Giesenhagen, H. C., Koppe, R., Hansen, H.-P., and Gocke, K.: Impact of change in climate and policy from 1988 to 2007 on environmental and microbial variables at the time series station Boknis Eck, Baltic Sea, Biogeosciences, 10, 4529–4546, doi:10.5194/bg-10-4529-2013, 2013.

IPCC: Climate Change 2013 – The Physical Science Basis, Contribution of Working Group I to the Fifth Assessment Report of the Intergovernmental Panel on Climate Change, edited by: Stocker, T. F., Qin, D., Plattner, G., Tignor, M., Allen, S., Boschung, J., Nauels, A., Xia, Y., Bex, V., and Midgley, P. M., Cambridge University Press, 2013.

Jackson, D. R., Williams, K. L., Wever, T. F., Friedrichs, C. T., and Wright, L. D.: Sonar evidence for methane ebullition in Eckernförde Bay, Cont. Shelf Res., 18, 1893–1915, 1998

Jähne, B., Heinz, G., and Dietrich, W.: Measurement of the diffusion coefficients of sparingly soluble gases in water, J. Geophys. Res.-Oceans, 92, 10767–10776, 1987.

James, R. H., Bousquet, P., Bussmann, I., Haeckel, M., Kipfer, R., Leifer, I., Niemann, H., Ostrovsky, I., Piskozub, J., Rehder, G., Treude, T., Vielstädte, L., and Greinert, J.: Effects of climate change on methane emissions from seafloor sediments in the Arctic, Limnol. Oceanogr., 61, S283–S299, doi:10.1002/lno.10307, 2016.

Judd, A. and Hovland, M.: Seabed Fluid Flow: The impact of geology, biology and the marine environment, Cambridge University Press, 2007.

Kalyuzhnaya, M. G., Yang, S., Rozova, O. N., Smalley, N. E., Clubb, J., Lamb, A., Nagana Gowda, G. A., Raftery, D., Fu, Y., Bringel, F., Vuilleumier, S., Beck, D. A. C., Trotsenko, Y. A., Khmelenina, V. N., and Lidstrom, M. E.: Highly efficient methane biocatalysis revealed in a methanotrophic bacterium, Nat. Commun., 4, p. 2785, 2013.

Keeling, R. F., Körtzinger, A., and Gruber, N.: Ocean deoxygenation in a warming world, Annu. Rev. March Sci., 2, 199–229, 2010.

Kessler, J. D., Valentine, D. L., Redmond, M. C., Du, M., Chan, E. W., Mendes, S. D., Quiroz, E. W., Villanueva, C. J., Shusta, S. S., Werra, L. M., Yvon–Lewis, S. A., and Weber, T. C.: A persistent Oxygen Anomaly Reveals the Fate of Spilled Methane in the Deep Gulf of Mexico, Science, 331, 312–315, 2011.

Kirschke, S., Bousquet, P., Ciais, P., Saunois, M., Canadell, J. G., Dlugokencky, E. J., Bergamaschi, P., Bergmann, D., Blake, D. R. Bruhwiler, L., Cameron-Smith, P., Castaldi, S., Chevallier, F., Feng, L., Fraser, A., Heimann, M., Hodson, E. L., Houweling, S., Josse, B., Fraser, P. J., Krummel, P. B., Lamarque, J.-F., Langenfelds, R. L., Le Quéré, C., Naik, V., O'Doherty, S., Palmer, P. I., Pison, I., Plummer, D., Poulter, B., Prinn, R. G., Rigby, M., Ringeval, B., Santini, M., Schmidt, M., Shindell, D. T., Simpson, I. J., Spahni, R., Steele, L. P., Strode, S. A., Sudo, K., Szopa, S., van der Werf, G. R., Voulgarakis, A., van Weele, M., Weiss, R. F., Williams, J. E., and and Zeng, G.: Three decades of global methane sources and sinks, Nat. Geosci., 6, 813–823, 2013.

Knittel, K. and Boetius, A.: Anaerobic Oxidation of Methane: Progress with an Unknown Process, Annu. Rev. Microbiol., 63, 311–334, 2009.

Lennartz, S. T., Lehmann, A., Herrford, J., Malien, F., Hansen, H.-P., Biester, H., and Bange, H. W.: Long-term trends at the Boknis Eck time series station (Baltic Sea), 1957–2013: does climate change counteract the decline in eutrophication?, Biogeosciences, 11, 6323–6339, doi:10.5194/bg-11-6323-2014, 2014.

Madigan, Q. D., Martinko, J., Bender, K., Buckley, D., and Stahl, D.: Brock Biology of Microorganisms, 13th edition, Pearson Education, San Francisco, 2015.

Maltby, J.: Production of greenhouse gases in organic-rich sediments, Ph. D. thesis, Christian-Albrechts-Universität, Kiel, Germany, 170 pp., http://oceanrep.geomar.de/id/eprint/30301 (last access: 30 Oktober 2016), 2015.

Mau, S., Heintz, M. B., and Valentine, D. L.: Quantification of CH_4-loss and transport in dissolved plumes of the Santa Barbara Channel, California, Cont. Shelf Res., 32, 110–120, 2012.

Mau, S., Blees, J., Helmke, E., Niemann, H., and Damm, E.: Vertical distribution of methane oxidation and methanotrophic response to elevated methane concentrations in stratified waters of

the Arctic fjord Storfjorden (Svalbard, Norway), Biogeosciences, 10, 6267–6278, doi:10.5194/bg-10-6267-2013, 2013.

Mau, S., Gentz, T., Körber, J.-H., Torres, M. E., Römer, M., Sahling, H., Wintersteller, P., Martinez, R., Schlüter, M., and Helmke, E.: Seasonal methane accumulation and release from a gas emission site in the central North Sea, Biogeosciences, 12, 5261–5276, doi:10.5194/bg-12-5261-2015, 2015.

Middelburg, J. J. and Levin, L. A.: Coastal hypoxia and sediment biogeochemistry, Biogeosciences, 6, 1273–1293, doi:10.5194/bg-6-1273-2009, 2009.

Milucka, J., Kirf, M., Lu, L., Krupke, A., Lam, P., Littmann, S., Kuypers, M. M. M., and Schubert, C. J.: Methane oxidation coupled to oxygenic photosynthesis in anoxic waters, ISME J., 9, 1991–2002, 2015.

Mohrholz, V., Naumann, M., Nausch, G., Krüger, S., and Gräwe, U.: Fresh oxygen for the Baltic Sea, An exceptional saline inflow after a decade of stagnation, J. Marine Syst., 148, 152–166, 2015.

Murrell, J. C.: The Aerobic Methane Oxidizing Bacteria (Methanotrophs), in: Handbook of Hydrocarbon and Lipid Microbiology, edited by: Timmis, K. N., Springer Berlin Heidelberg, 1953–1966, 2010.

Naqvi, S. W. A., Bange, H. W., Farías, L., Monteiro, P. M. S., Scranton, M. I., and Zhang, J.: Marine hypoxia/anoxia as a source of CH_4 and N_2O, Biogeosciences, 7, 2159–2190, doi:10.5194/bg-7-2159-2010, 2010.

Nausch, G., Naumann, M., Umlauf, L., Mohrholz, V., and Siegel, H.: Hydrographisch-hydrochemische Zustandseinschätzung der Ostsee 2013, Leibniz-Institut für Ostseeforschung Warnemünde, Meereswiss. Ber. (Mar. Sc. Rep.), doi:10.12754/msr-2014-0093, 2014.

Nauw, J., Haas, H. D., and Rehder, G.: A review of oceanographic and meteorological controls on the North Sea circulation and hydrodynamics with a view to the fate of North Sea methane from well site 22/4b and other seabed sources, March Petrol. Geol., 68, 861–882, 2015.

Niemann, H., Steinle, L. I., Blees, J., Krause, S., Bussmann, I., Treude, T., Krause, S., Elvert, M., and Lehmann, M. F.: Toxic effects of butyl elastomers on aerobic methane oxidation, Limnol. Oceanogr.-Meth., 13, 40–52, 2015.

Osudar, R., Matoušů, A., Alawi, M., Wagner, D., and Bussmann, I.: Environmental factors affecting methane distribution and bacterial methane oxidation in the German Bight (North Sea), Estuar. Coast. Shelf S., 160, 10–21, 2015.

Oswald, K., Milucka, J., Brand, A., Littmann, S., Wehrli, B., Kuypers, M. M., and Schubert, C. J.: Light-dependent aerobic methane oxidation reduces methane emissions from seasonally stratified lakes, PloS One, 10, e0132574, doi:10.1371/journal.pone.0132574, 2015.

Price, P. B. and Sowers, T.: Temperature dependence of metabolic rates formicrobial growth, maintenance, and survival, P. Natl. Acad. Sci. USA, 101, 4631–4636, 2014.

Prinn, R. G., Weiss, R. F., Fraser, P. J., Simmonds, P. G., Cunnold, D. M., O'Doherty, S., Salameh, P. K., Porter, L. W., Krummel, P. B., Wang, R. H. J., Miller, B. R., Harth, C., Greally, B. R., Van Woy, F. A., Steele, L. P., Mühle, J., Sturrock, G. A., Alyea, F. N., Huang, J., and Hartley, D. E.: The ALE/GAGE AGAGE Network, Carbon Dioxide Information Analysis Center (CDIAC), Oak Ridge National Laboratory (ORNL), US Department of Energy (DOE), 2013.

Rabalais, N. N., Cai, W.-J., Carstensen, J., Conley, D. J., Fry, B., Hu, X., Quiñones-Rivera, Z., Rosenberg, R., Slomp, C. P., Turner, R. E., Voss, M., Wissel, X., and Zhang, J.: Eutrophication-driven deoxygenation in the coastal ocean, Oceanography, 27, 172–183, 2014.

Raymond, P. A., and Cole, J. J.: Gas exchange in rivers and estuaries: Choosing a gas transfer velocity, Estuar. Coast., 24, 312–317, 2001.

Reeburgh, W. S.: Oceanic methane biogeochemistry, Chem. Rev., 107, 486–513, 2007.

Reeburgh, W. S., Ward, B. B., Whalen, S. C., Sandbeck, K. A., Kilpatrickt, K. A., and Kerkhof, L. J.: Black Sea methane geochemistry, Deep-Sea Res., 38, S1189–S1210, 1991.

Rehder, G., Keir, R. S., Suess, E., and Pohlmann, T.: The multiple sources and patterns of methane in North Sea waters, Aquat. Geochem., 4, 403–427, 1998.

Rhein, M., Rintoul, S. R., Aoki, S., Campos, E., Chambers, D., Feely, R. A., Gulev, S., Johnson, G. C., Josey, S. A., Kostianov, A., Mauritzen, C., S. Gulev, S. Johnson, G.C. Josey, S. A. Kostianoy, A. Mauritzen, C. Roemmich, D., Talley, L. D., and Wang, F.: Observations: Oceans, in: I.P.O.C. Change, Climate Change 2013 – The Physical Science Basis, Cambridge University Press, 255–316, 2013.

Schmale, O., Schneider von Deimling, J., Gülzow, W., Nausch, G., Waniek, J. J., and Rehder, G.: Distribution of methane in the water column of the Baltic Sea, Geophys. Res. Lett., 43, 5225–5232, doi:10.1029/2010GL043115, 2010.

Schubert, C. J., Coolen, M. J., Neretin, L. N., Schippers, A., Abbas, B., Durisch–Kaiser, E., Wehrli, B., Hopmanns, E. C., Sinninghe Damsté, J. S., Wakeham, S., and Kuypers, M. M. M.: Aerobic and anaerobic methanotrophs in the Black Sea water column, Environ. Microbiol., 8, 1844–1856, 2006.

Siedler, P. and Peters, H.: Properties of sea water, Physical properties (general), in: Landolt-Börnstein, Numerical Data and Functional Relationships in Science and Technology, edited by: Sündermann, J., New Series, Oceanography, Springer Verlag, 233–264, 1986.

Smetacek, V.: The annual cycle of Kiel Bight plankton: a long-term analysis, Estuaries, 8, 145–157, 1985.

Smetacek, V., von Bodungen, B., Knoppers, B., Peinert, R., Pollehne, F., Stegmann, P., and Zeitzschel, B.: Seasonal stages characterizing the annual cycle of an inshore pelagic system, Rapports et Proces-Verbaux des Reunions Conseil International pour L'Exploration de la Mer, 183, 126–135, 1984.

Steinle, L., Graves, C. A., Treude, T., Ferré, B., Biastoch, A., Bussmann, I., Berndt, C., Krastel, S., James, R. H., Behrens, E., Böning, C. W., Greinert, J., Sapart, C.-J., Scheinert, M., Sommer, S., Lehmann, M., F., and Niemann, H.: Water column methanotrophy controlled by a rapid oceanographic switch, Nat. Geosci., 8, 378–382, 2015.

Steinle, L., Schmidt, M., Bryant, L., Haeckel, M., Linke, P., Sommer, S., Zopfi, J., Lehmann, M. F., Treude, T., and Niemann, H.: Linked sediment and water column methanotrophy at a man-made gas blowout in the North Sea: Implications for methane budgeting in seasonally stratified shallow seas, Limnol. Oceanogr., 61, S367–S368, doi:10.1002/lno.10388, 2016.

Steinle, L., Maltby, J., Treude, T., Kock, A., Bange, H. W., and Niemann, H.: Physico-chemical data including methane concentrations, as well as methane oxidation rates, measured at time-series

station Boknis Eck (Baltic Sea) from 2012–2014, PANGAEA, doi:10.1594/PANGAEA.871890, 2017.

Stolper, D. A., Revsbech, N. P., and Canfield, D. E.: Aerobic growth at nanomolar oxygen concentrations, P. Natl. Acad. Sci. USA, 107, 18755–18760, 2010.

Treude, T., Krüger, K., Boetius, A., and Jørgensen, B.B.: Environmental control on anaerobic oxidation of methane in gassy sediments of Eckernförde Bay (German Baltic), Limnol. Oceanogr., 50, 1771–1786, 2005.

Upstill–Goddard, R. C., Barnes, J., Frost, T., Punshon, S., and Owens, N.J.: Methane in the southern North Sea: Low-salinity inputs, estuarine removal, and atmospheric flux, Global Biogeochem. Cy., 14, 1205–1217, 2000.

Upstill-Goddard, R. C. and Barnes, J.: Methane emissions from UK estuaries: Re-evaluating the estuarine source of tropospheric methane from Europe, Mar. Chem., 180, 14–23, 2016.

Whiticar, M. J.: Diagenetic relationships of methanogenesis, nutrients, acoustic turbidity, pockmarks and freshwater seepages in Eckernförde Bay, Mar. Geol., 182, 29–53, 2002.

Wiesenburg, D. A. and Guinasso Jr., N. L.: Equilibrium solubilities of methane, carbon monoxide, and hydrogen in water and sea water, J. Chem. Eng. Data, 24, 356–360, 1979.

Zopfi, J., Ferdelman, T. G., Jørgensen, B. B., Teske, A., and Thamdrup, B.: Influence of water column dynamics on sulfide oxidation and other major biogeochemical processes in the chemocline of Mariager Fjord (Denmark), Mar. Chem., 74, 29–51, 2001.